

# Image Registration Based on Fast Fourier Transform Using Gabor Filter

R. Kokila, and P. Thangavel

**Abstract**—Image registration is essential in image processing applications especially in the medical field. CT, X-ray and MRI medical images play a pivotal role in clinical and medical research. In order to register smaller images such as tumor or fractures in an image, we propose a Gabor filter based medical image registration technique, that detects translation, scale and rotation parameters between the images. The proposed scheme is tested on the face dataset. Experimental results show that the proposed method works better and faster than normalised gradient correlation (NGC) based method.

**Keywords**—Gabor filter, Fast Fourier transform, Log polar transform, Image registration, Phase correlation.

## I. INTRODUCTION

REGISTRATION of two dimensional images acquired from the same scene taken at different times, from different geometric viewpoint, or by a different image sensor is a fundamental problem in the image processing. Image registration is the preprocessing step for the analysis and fusion of the images. Image mosaicing, super resolution and the fusion of multimodal images like remote sensing, medical imaging and computer vision are the typical application for the image registration.

The main objective of image registration is to find the geometric transformation of the source image  $I^S$ , to the target image  $I^T$ , where  $I^T(x, y) = \tau\{I^S(x', y')\}$  and  $\tau$  is two dimensional geometric transformation that associates the  $(x', y')$  co-ordinate in  $I^S$  with  $(x, y)$  co-ordinate in  $I^T$ . The two dimensional geometric transformation includes scale, rotation and translation in the cartesian co-ordinate. Image registration can be broadly classified into area based and feature based methods. The feature based approach matches the features of salient details of the image, whereas the area based approach matches the whole image.

The source and target images differ from each other by its scale, rotation and translation that can be determined by using fast Fourier transform (FFT) method [12]. The Fourier method searches for the optimal match based on the information in the frequency domain. Because of this distinct feature it differs from other registration strategies. Matungaka et al. [11] proposed an adaptive polar transform with projection transform along with matching mechanism to recover the

scale, rotation and translation. Tzimiropoulos et al. [16] have reported FFT based registration scheme with image gradients. They replaced the image functions with the complex gray level edge maps and then performed FFT. Then resampled it on the log-polar grid and normalised gradient correlation (NGC) is used to detect the geometric transformations. Lin et al. [9] proposed a method for automatic registration. In this, they first applied Harris operator to extract the corner features after that Canny operator is implemented to detect the image edges. The correlation between the image pairs yields the corner points. The affine transformation between the image pair is established, which calculates the parameters, according to that the images are registered. Gonzalez [6] proposed a novel phase correlation technique to estimate the geometric transformation. Thangavel and Kokila [15] proposed an extension of FFT based image registration.

Manjunath and Ma [10] proposed the use of Gabor wavelet feature for the texture analysis. Lee [7] extended Daubechies' one dimensional wavelets to two dimensional for the frame criterion. It also computes the frame bounds for fractionally dilated two dimensional wavelets and frame bounds for various sampling scheme. Bařina and Zemřık [2] used Gabor wavelets as multiscale partial differential operator to detect the edges, corners and blobs. The performance of these interest point detector is compared to detectors utilizing Haar wavelets and a derivative of a Gaussian function.

Wu and Chung [17] proposed a novel and straight forward multimodal image registration method based on wavelet representation, in which two matching criteria are used including sum of absolute difference (SAD) for improving registration robustness and mutual information (MI) for assuring the registration accuracy. Serlie et al. [14] presented a fully automated method to classify three dimensional CT data into material functions. Liao and Chung [8] proposed a new feature based non-rigid image registration method for magnetic resonance (MRI) brain image. Roozgard et al. [13] proposed a dense registration technique by aligning local 3D features of two CT images using sparse coding and belief propagation.

In this paper, we propose Gabor filter based image registration. Gabor filter is applied to extract the impulse response from both the source and target image, to this phase correlation is applied in order to recover the geometric transformation between the images. The main objective of this registration scheme is to locate the target image in the source image, even when the target image is not located in the center region of the source image. The paper is organised as follows: in Section II we have described about Gabor filter in detail. Section III discusses about FFT based image registration.

R. Kokila is with the Department of Computer science, University of Madras, Chepauk, Chennai-600 005, India. (e-mail:kok\_oc25@yahoo.co.in).

P. Thangavel is with the Department of Computer science, University of Madras, Chepauk, Chennai-600 005, India. (Corresponding author's phone: 91-44-25399502; e-mail:thangavelp@yahoo.com).

Algorithm is presented in Section IV. Experimental results are described in Section V. Conclusion is drawn in Section VI.

## II. GABOR FILTER

In this section we review about Gabor filter. A one dimensional Gabor filter was proposed by Hungarian born scientist Dennis Gabor in 1946 [5]. Daugman [4] extended one dimensional Gabor filter to two dimension. Gabor filters have been used in many applications, such as texture segmentation, target detection, fractal dimension management, document analysis, edge detection, retina identification, image coding and image representation. The filter has a real and an imaginary component representing orthogonal directions. The two components may be formed into a complex number or used individually. The Gabor filter is constructed using the following equation:

Complex

$$g(x, y, f, \theta) = e^{-\frac{1}{2}\left(\frac{(x')^2}{\sigma_x^2} + \frac{(y')^2}{\sigma_y^2}\right)} \times e^{j2\pi f x'}$$

Real

$$g(x, y, f, \theta) = e^{-\frac{1}{2}\left(\frac{(x')^2}{\sigma_x^2} + \frac{(y')^2}{\sigma_y^2}\right)} \times \cos(2\pi f x')$$

Imaginary

$$g(x, y, f, \theta) = e^{-\frac{1}{2}\left(\frac{(x')^2}{\sigma_x^2} + \frac{(y')^2}{\sigma_y^2}\right)} \times \sin(2\pi f x')$$

where

$$\begin{aligned} x' &= x \cos \theta + y \sin \theta \\ y' &= -x \sin \theta + y \cos \theta \end{aligned}$$

In these equations,  $x$  and  $y$  specify the position of the light impulse in the visual field,  $\theta$  is the orientation of the Gabor filter,  $f$  is the frequency of sinusoidal plane wave,  $\sigma_x$  and  $\sigma_y$  control the sharpness of the filter on the major and minor axes respectively.

## III. FOURIER TRANSFORM BASED IMAGE REGISTRATION

In this section we review the Fourier transform theory for image registration [12], [16].

### A. Translation

A displacement  $(x_0, y_0)$  between two images  $f_1$  and  $f_2$  are related as follows:

$$f_2(x, y) = f_1(x - x_0, y - y_0)$$

$F_1$  and  $F_2$  the Fourier transforms of  $f_1$  and  $f_2$  respectively, are related as follows:

$$F_2(\omega_1, \omega_2) = F_1(\omega_1, \omega_2) * e^{-2\pi j(\omega_1 x_0 + \omega_2 y_0)}$$

The corresponding crosspower spectrum of the Fourier transforms,  $F_1$  and  $F_2$  is defined as follows:

$$\frac{F_2(\omega_1, \omega_2) F_1^*(\omega_1, \omega_2)}{|F_2(\omega_1, \omega_2) F_1(\omega_1, \omega_2)|} = e^{-2\pi j(\omega_1 x_0 + \omega_2 y_0)}$$

Here  $F_1^*$  is the complex conjugate of  $F_1$ . The phase of crosspower spectrum is equivalent to the phase difference between the two images, guaranteed by the shift theorem. The inverse Fourier transform is applied to the result of the crosspower spectrum, produces an impulse function, that is approximately zero everywhere except at the point of displacement. The location of the impulse function is used to register the two images.

### B. Rotation

Let  $f_2$  be a translated and rotated image of  $f_1$  by  $(x_0, y_0)$  and  $\theta_0$  respectively, and written as:

$$f_2(x, y) = f_1\left(\begin{matrix} x \cos \theta_0 + y \sin \theta_0 - x_0, \\ -x \sin \theta_0 + y \cos \theta_0 - y_0 \end{matrix}\right)$$

According to the properties of Fourier transforms,  $F_1$  and  $F_2$ , the transforms of  $f_1$  and  $f_2$  respectively, are related as follows:

$$F_2(\omega_1, \omega_2) = F_1\left(\begin{matrix} \omega_1 \cos \theta_0 + \omega_2 \sin \theta_0, \\ -\omega_1 \sin \theta_0 + \omega_2 \cos \theta_0 \end{matrix}\right) * e^{-2\pi j(\omega_1 x_0 + \omega_2 y_0)}$$

If the magnitude of  $F_1$  and  $F_2$  are denoted as  $M_1$  and  $M_2$  respectively, the above equation can be rewritten as:

$$M_2(\omega_1, \omega_2) = M_1\left(\begin{matrix} \omega_1 \cos \theta_0 + \omega_2 \sin \theta_0, \\ -\omega_1 \sin \theta_0 + \omega_2 \cos \theta_0 \end{matrix}\right)$$

The magnitudes of  $M_1$  and  $M_2$  are converted to polar coordinates, then the Phase correlation is applied to determine the rotation ( $\theta_0$ )

$$M_1(\rho, \theta) = M_2(\rho, \theta - \theta_0)$$

### C. Scale

When an image is scaled by scale factor  $a$ , the relation between the Fourier transform of the image and its scaled image is expressed as follows:

$$F_2(\omega_1, \omega_2) = \frac{1}{a^2} F_1\left(\frac{\omega_1}{a}, \frac{\omega_2}{a}\right)$$

The above equation can be rewritten in the logarithmic domain as follows:

$$F_2(\log \omega_1, \log \omega_2) = F_1(\log \omega_1 - \log a, \log \omega_2 - \log a)$$

From the above equation, we can find the scale factor  $a$ . Here constant  $\frac{1}{a^2}$  is ignored for simplicity.

### D. Translation, rotation and scale

When the given two images differ each other with translation, rotation and scaling, their corresponding magnitude spectrum can be represented as follows:

$$M_2(\rho, \theta) = M_1\left(\frac{\rho}{a}, \theta - \theta_0\right)$$

The respective magnitudes in the log polar co-ordinate system are related as follows:

$$M_2(\log \rho, \theta) = M_1(\log \rho - \log a, \theta - \theta_0)$$

The Fourier phase shifting property is used to recover the rotation and scaling between the two images. Once rotation and scaling parameters are recovered then these parameters are applied to image  $f_2$ . Now the translational offset between  $f_1$  and  $f_2$  are obtained by applying the standard phase correlation technique.

#### E. Highpass filter

The Fourier magnitude spectra are represented in the log polar domain. They are then multiplied with the highpass emphasis filter. Here the transfer function used is:

$$HPF(\xi, \eta) = (1.0 - X(\xi, \eta)) * (2.0 - X(\xi, \eta))$$

where

$$X(\xi, \eta) = [\cos(\pi\xi) \cos(\pi\eta)] \text{ and } -0.5 \leq \xi, \eta \leq 0.5$$

#### F. Log-Polar Transform

In image processing, Log-polar transform (LPT) is a well known tool, because of its scale and rotation invariant properties. It is a nonlinear and non-uniform sampling method, used to convert an image from the cartesian co-ordinate to the polar co-ordinate. The mapping procedure is as follows:

$$\rho = \log_{base} \sqrt{(x - x_c)^2 + (y - y_c)^2}$$

$$\theta = \tan^{-1} \frac{(y - y_c)}{(x - x_c)}$$

Here,  $(x_c, y_c)$  is the center pixel of the transformation in the cartesian co-ordinate.  $(x, y)$  Denotes the sample pixel in the cartesian co-ordinate and  $(\rho, \theta)$  denotes the log radius and angular position in the log polar co-ordinate. We have used the natural logarithm. The log polar co-ordinate is used instead of cartesian co-ordinate, because the scale and rotation in the cartesian co-ordinate is represented as a shift in the log radius and angular directions in the log-polar co-ordinates respectively. For example, Fig. 1 shows the source image, target image, LPT of source image and LPT of target image.

#### IV. ALGORITHM

In this section, the detailed algorithm for Gabor filter based medical image registration scheme is presented.

Input: Let  $f_1$  and  $f_2$  be source and target images respectively

- 1) The impulse response of the source and target images are determined by using Gabor filter and then Tukey window function is applied. Zeropad both target and source images, so that the image will be of size  $N \times N$  where  $N = 2^n$  such that

$N \geq \max(\text{size}(f_1), \text{size}(f_2))$  and  $n$  is the smallest integer.

- 2) Forward fast Fourier transform is applied on the computed impulse response of  $f_1$  and  $f_2$ , denoted as  $F_1$  and  $F_2$  respectively. Now magnitude  $M_1$  and  $M_2$  are calculated from  $F_1$  and  $F_2$ .
- 3) The Fourier log magnitude spectra  $M_1$  and  $M_2$  are multiplied with Highpass emphasis filter.
- 4) The resulting spectra is resampled on the log polar co-ordinates.
- 5) Scale factor and rotation angle are calculated using phase correlation technique on the log-polar Fourier magnitude spectra of both the images.
- 6) Calculated scale factor and rotation angle are applied to the target image and once again the phase correlation technique is performed in order to detect the translational offset between the source and target image.

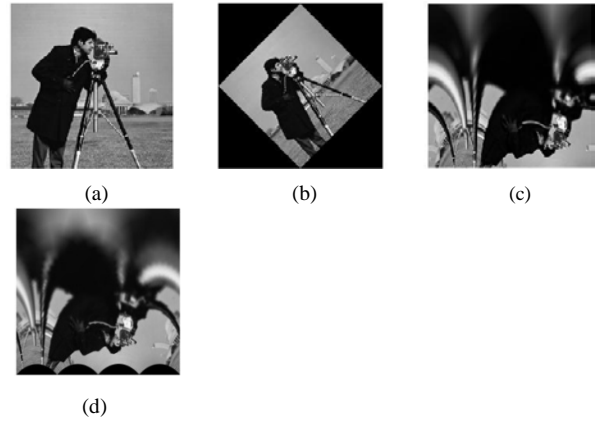


Fig. 1. (a) Source Image (b) Target Image (scaled with 1.2 and rotated with 45°) (c) LPT of Source Image (d) LPT of Target Image

#### V. EXPERIMENTAL RESULTS

Gabor filter is applied as the preprocessing task in order to retrieve the impulse response of the source and target image. To extract the impulse response from an image, a Gabor filter with  $\sigma_x = 2$  and  $\sigma_y = 2$ , rotation with 45° and frequency 2 is utilized. Using the above parameter list, the Gabor filter is constructed. It is then convolved with the image to produce the impulse response of the source and target images, then the Tukey window function is applied. Zeropad the impulse response of Tukey windowed image of size  $N \times N$  where  $N = 2^n$  such that  $N \geq \max(\text{size}(f_1), \text{size}(f_2))$  and  $n$  is small integer. Then two dimensional Fourier transform of both images are computed, to determine the Fourier spectra. The highpass filter with the transfer function is constructed. The Fourier log magnitude spectra is multiplied with highpass emphasis filter. The resulting spectrum is resampled to log polar co-ordinates by using by using  $base = \exp(\log(\frac{N}{2}) * \frac{2}{N})$  as a logarithmic base on the log polar domain along with radial axis. In order to detect the location of the translation, phase correlation is applied on the transformed images of

source and target. The location of translation will be either at  $x$  or  $N-x$ , on the basis of which image has higher resolution. The scale and rotation can be calculated using the following formulas,  $scale = \exp(\log(\frac{N}{2}) * \frac{2}{N} * x)$  and  $\theta_0 = \frac{180 * y}{N/2}$ . When the rotation is to be determined,  $180^\circ$  ambiguity arises. This can be solved as follows: Let the determined angle be  $\theta_0$ . Now rotate the spectra of source image by determined angle ( $\theta_0$ ), simultaneously rotate the spectrum of source image by  $(180^\circ + \theta_0)$  and again locate the translation. At angle  $\theta_0$ , if the peak value of the inverse Fourier transform of the crosspower spectrum is greater, then the true angle of the rotation is  $\theta_0$ , otherwise it is  $(180^\circ + \theta_0)$ . The computed scale factor and rotation angle are applied to the target image.

TABLE I  
THE DETECTION RATIO FOR EACH SCALE (S) RANGE FOR THE SELECTED IMAGE DATASET, USING GABOR FILTER BASED SCHEME.

Image	$S \leq 2$	$2 < S \leq 4$	$4 < S \leq 6$	$6 < S \leq 8$
CT-1	11/11	20/20	20/20	20/20
CT-5	11/11	19/20	19/20	20/20
CT-6	11/11	20/20	20/20	20/20
CT-8	11/11	20/20	20/20	20/20
CT-9	11/11	20/20	20/20	20/20
CT-12	11/11	20/20	20/20	20/20
MRI-1	11/11	20/20	19/20	8/20
MRI-2	11/11	20/20	20/20	5/20
MRI-6	11/11	18/20	19/20	0/20
MRI-8	11/11	20/20	20/20	5/20
MRI-16	11/11	20/20	17/20	2/20
MRI-20	11/11	18/20	20/20	2/20
Ivp-xray	11/11	20/20	20/20	20/20
Abdo-lower	11/11	20/20	20/20	20/20
Xray-hand	11/11	20/20	20/20	20/20
Xray-spine	10/11	17/20	6/20	2/20
Vcug	11/11	20/20	20/20	20/20
over all	186/187	332/340	320/340	224/340

If the computed scale factor and rotation angle are not able to register the source image with the target image, then rotate the target image in anticlockwise direction with  $50^\circ$  and then apply the proposed method to detect the geometric transformation. Once the scale factor and rotation angle are determined, the rotation angle is added with  $50^\circ$ . Now scale down the scale factor and rotate the target image with determined geometric transformation and then perform phase correlation to detect the translation.

#### A. Performance evaluation on Medical images

To evaluate the performance of the proposed Gabor filter based image registration scheme, we have conducted experiments on different sets of CT images, MRI images, X-ray images, angiogram of eye and some disease images of Squamous Carcinoma, Gangrene of Finger and Toe respectively.

We have conducted experiments on different datasets to test the performance of our method to detect scale, rotation and translation solely and the results are shown in Table I. We have divided the scale factor into four different components as

follows:  $S \leq 2$ ,  $2 < S \leq 4$ ,  $4 < S \leq 6$  and  $6 < S \leq 8$ . For each dataset, we have computed total number of registrations,

$$\text{Total No. of registration} = \frac{\text{No. of image pairs registered}}{\text{No. of image pairs tested}}$$

TABLE II  
COMPARISON OF MAXIMUM SCALE FACTOR FOR EACH IMAGE PAIR WITH FAST FOURIER TRANSFORM (FFT), NORMALISED GRADIENT CORRELATION (NGC) AND GABOR FILTER BASED METHODS

Image	FFT	NGC	Gabor Filter
	Scale	Scale	Scale
CT-Tumor	1.44	2.43	3.40
Tumor-F13	0	0	2.78
Lung cancer	1.23	2.99	6.48
Hand-screw	1.46	2.23	3.38
Hand	1.8	3	3.34
Broken-knee	1	1	4.11
Mr-images	1.10	1.41	2.71
Knee-tumor	1	1	2.71
Spline-tumor	1	1.30	5.08

The overall total number of image pairs registration is given in the last row. Our proposed scheme performed well on CT images where as for MRI images it yielded less number of registrations when the scale lies between 6 to 8, whereas in Xray-spine image out of 20 images it registered only 6 and 2 images when the scale range between 4 to 6 and 6 to 8 respectively.

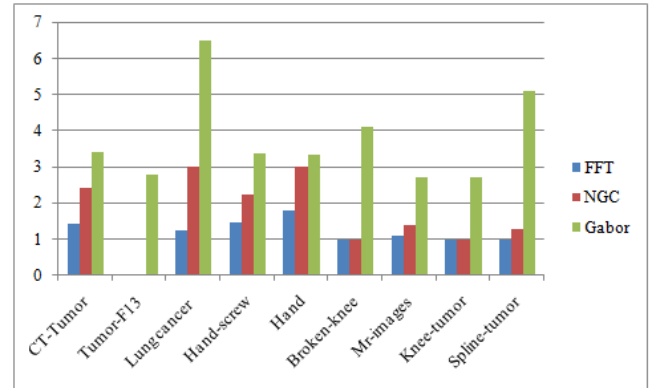


Fig. 2. Comparison of maximum scale factor registered using Fast Fourier transform (FFT), normalised gradient correlation (NGC) and Gabor filter based schemes for different image pairs.

In order to compare the effectiveness of maximum scale factor between the proposed method, NGC based method and FFT method, we have used three different CT images with tumors, three different MRI images with tumors and three X-ray images with fractures. We tried to register the tumors in CT and MRI images. The X-ray images were used to detect the fracture area in the source image. NGC based method and FFT method perform well only when the tumor or fractured area is present in the center region of the source image. Because of this problem, for Tumor-F13 image, NGC based method was not able register the source image with target image, for Broken-knee and Knee-tumor beyond the scale 1.

Its corresponding pictorial representation and tabular values of the maximum scale factor comparison between NGC based method, FFT method and Gabor filter based method are shown in Fig. 2 and Table II. In particular, for the Lung cancer image of size  $585 \times 429$  and its Tumor size  $148 \times 133$ , the NGC based method was able to register up to 2.99 scale, FFT method registered up to the scale factor of 1.23 where as the proposed Gabor filter based method is able to register up to 6.48 scaling factor. From this table, we can conclude that the Gabor filter based method can register smaller size images than NGC based method and FFT method.

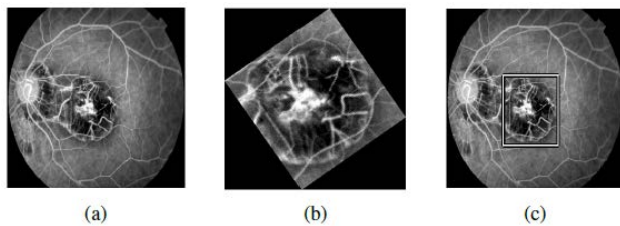


Fig. 3. Image registration result using the proposed approach on the Cornea Retina scar image (a) Source Image (b) Target Image (scaled 6.5 times and rotated  $35^\circ$ ) (c) Registration result using the proposed approach.

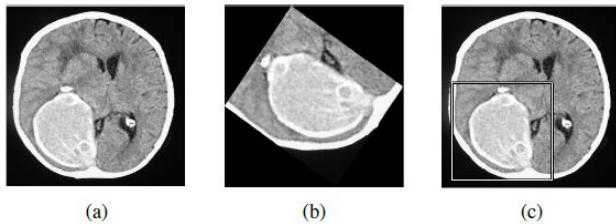


Fig. 4. Image registration result using the proposed approach on the CT-Tumor image (a) Source Image (b) Target Image (scaled 3.4 times and rotated  $55^\circ$ ) (c) Registration result using the proposed approach.

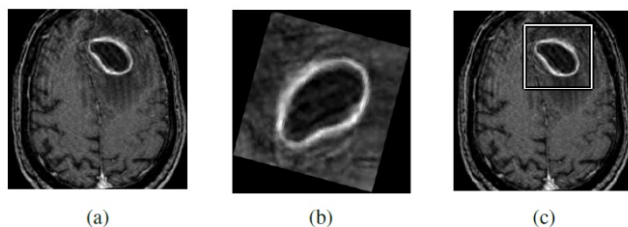


Fig.5. Image registration result using the proposed approach on the Mr-images image (a) Source Image (b) Target Image (scaled 2.7 times and rotated  $75^\circ$ ) (c) Registration result using the proposed approach.

The registration results on the selected set of images using the proposed approach are shown in Fig. 3 – 5. Each figure consists of three subfigures. The subfigure on the left is the source image and the subfigure in the middle is the target image which is to be registered with the source image. The subfigure on the right is the registered image using proposed image registration method.

Gabor filter detects the impulse response of the image. Medical image does not contain rich detail of the information, when we want to register the small image in the large image it will be difficult in NGC based method. To overcome this

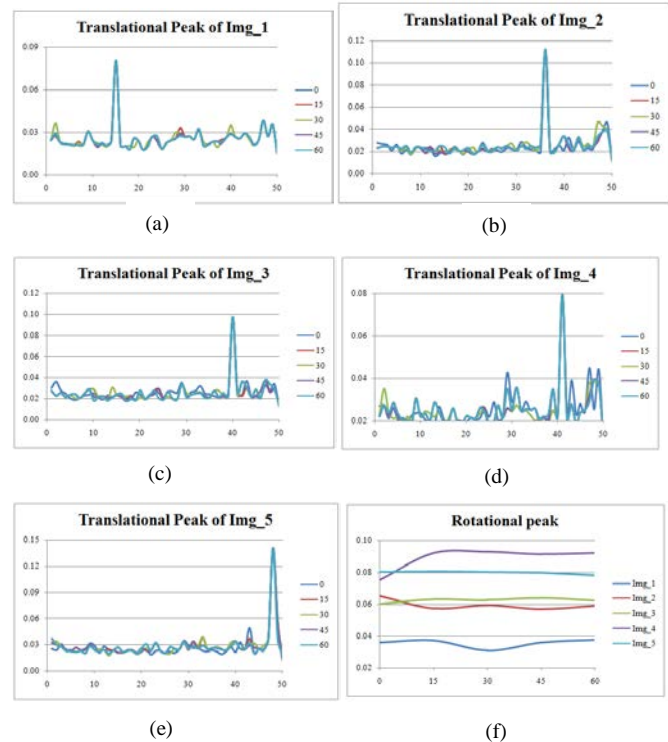


Fig. 6. Translational and Rotational impulse peak of proposed scheme on medical images; for different  $\theta$ -values of Gabor filter.

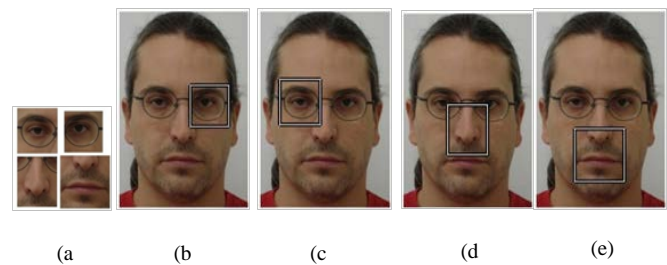


Fig. 7. Image registration result using the proposed approach on the Color image of Face – 5 image (a) Target Image (b) - (e) Registration result.

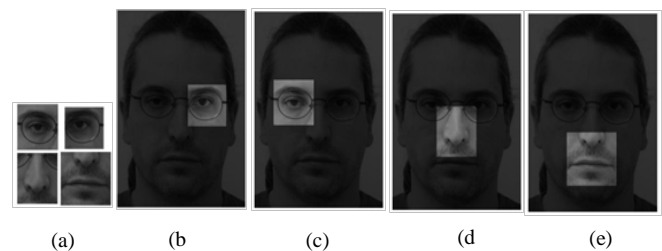


Fig. 8. Image registration result using the proposed approach on the Grayscale image of Face – 5 image (a) Target Image (b) - (e) Registration result.

problem, we have used Gabor filter to detect the impulse response of the image and that is used to register the image pairs. We designed Gabor filter with  $\sigma_x = 2$  and  $\sigma_y = 2$ ,



rotation with  $0^\circ, 15^\circ, 30^\circ, 45^\circ, 60^\circ$  and frequency with  $f = 2$ . We carried out the experiment on the medical image images in order to locate the tumor in the CT image dataset which consists of 50 images. Each source image will give translational peak for different  $\theta$  value and that is plotted in Fig. 6. The highest translational peak for different  $\theta$  resulted in the same peak value that is shown in Fig. 6(a) - Fig. 6(e) but their corresponding rotational peak differs for different  $\theta$  values and their pictorial representation is shown in Fig. 6 (f).

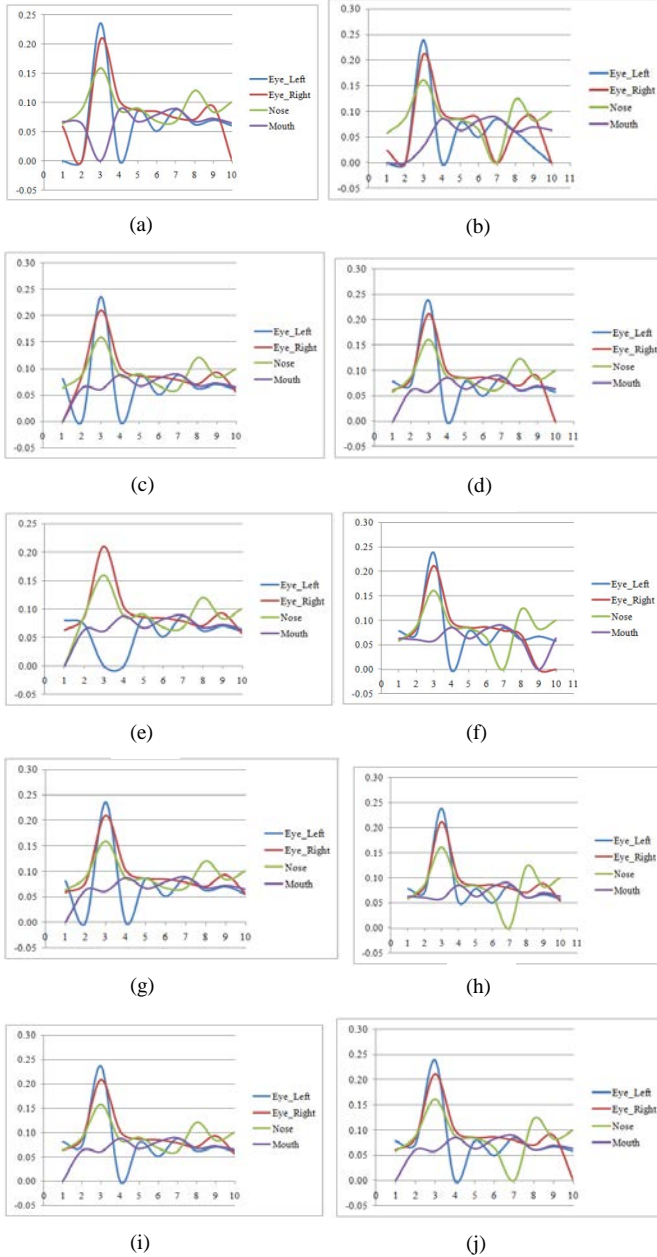


Fig. 9. Translational impulse peak of proposed scheme on face dataset:  $\theta = 0^\circ, 15^\circ, 30^\circ, 45^\circ, 60^\circ$  color images are (a), (c), (e), (g), (i) and grayscale images are (b), (d), (f), (h), (j)

Maximum rotational peak value for *Img - 5* was at  $\theta = 15^\circ$ ; *Img - 2*, *Img - 4* were at  $\theta = 30^\circ$ ; *Img - 3* was at  $\theta = 45^\circ$ ; *Img - 1* was at  $\theta = 60^\circ$ . From this we can conclude

that mostly maximum translational peak is found  $\theta \geq 30^\circ$ , so we have used  $\theta = 45^\circ$  for registering medical images using Gabor filter.

#### B. Performance evaluation on Facial images

We have performed experiments on a dataset of frontal views of human face, which consists of 100 face images. We carried out experiments on both the gray scale images and color images. In the grayscale image, left eye from *Face - 5* image is cropped and used as the target image and we tried to match and register it on the appropriate person's face. We applied our proposed method to the source and target image. Each source image will give the translational impulse peak. We have used the maximum translational impulse peak, and the corresponding geometric transformation to register the source and target image.

For the color image, first we apply the proposed scheme on the red band of the 100 source images and 1 target image, and then on Green and Blue band images. Each band image will have translational peak and rotational peak. In particular, left eye of *Face - 10* image is used as target image. After applying the proposed registration method, then we find the maximum translation peak among them. The highest translation peak of Red, Green, Blue are 0.0529, 0.0508, 0.0495 and their corresponding rotational peaks are 0.0301, 0.0427, 0.0410 respectively. Now we have to determine maximum translation among the three band, Red image will give us highest translation peak and their corresponding registered image result was *Face - 15* it is a mismatch registration result, in order to overcome the problem we need to find the maximum rotational peak among highest translational peak, highest rotational peak is 0.0427 on Green band image, their corresponding scale and rotation are used to register the source with target image. Each source image will yield the translational and rotational peak. We have to find the maximum translational peak on the red, green and blue bands, then determine the maximum rotational peak among the maximum translational peak. The corresponding geometric transformations are used to register the source image with the target image. The color and grayscale image registration results of *Face - 5* are shown in Fig. 7 and Fig. 8 respectively.

We have used design Gabor filter with  $\sigma_x = 2$ ,  $\sigma_y = 2$ , rotated with different  $\theta = 0^\circ, 15^\circ, 30^\circ, 45^\circ, 60^\circ$  and frequency with  $f = 2$  on face dataset which consists of 100 face image. At  $\theta = 0^\circ$  color image based image registration scheme gave us 4 mismatch registration results where as grayscale based image registration scheme gave us 6 mismatch registration results out of 40 images. Similarly for  $\theta = 15^\circ, 30^\circ, 45^\circ, 60^\circ$ , color image and grayscale image based registration scheme resulted in mismatch registration with 4 and 3; 4 and 5; 3 and 1; 2 and 4 respectively. For color images, at  $\theta = 0^\circ, 30^\circ, 60^\circ$  gave us better registration results than at  $\theta = 15^\circ, 45^\circ$ . It was vice versa for grayscale image. Their registration results are shown in Fig. 9.

Matlab R2010b running on 2.30GHz Intel core (TM) ma-

chine is used to perform all the experiments.

## VI. CONCLUSION

In this paper we have presented FFT based image registration using Gabor filter. Gabor filter detects the impulse response that do not lose any necessary information. Using Gabor filter based method we were able to register even the smaller size images. Experiments were conducted to locate the tumor and fracture in CT and MRI images and X-ray images respectively and attained better results. We compared our results with NGC method [16] and found the Gabor filter based method performs better than NGC based method even when the target image is not in the center region of the source image. We have carried out the experiments with face dataset of 100 images on both color and grayscale image to test the accuracy of the proposed method. The proposed method is able to register the source image with target image up to the scale factor of 8.

## ACKNOWLEDGMENT

This work is partially supported by University Grant Commission Major Research Project, Government of India.

## REFERENCES

- [1] G. Amayeh, A. Tavakkoli and G. Bebis, "Accurate and efficient computation of Gabor features in real-time applications," *Proc. Advances in Visual Computing*, vol. 5875, Springer Berlin Heidelberg, pp. 243–252, 2009.
- [2] D. Bařina, and P. Zemřık, "Gabor wavelets in image processing," Technical report, Brno University of Technology, 2011.
- [3] D. Casasent and D. Psaltis, "Position oriented and scale invariant optical correlation," *Appln. Opt.*, vol. 15, pp. 1793–1799, 1976.
- [4] J. Daugman, "Uncertainty relation for resolution in space, spatial frequency, and orientation optimized by two-dimensional visual cortical filters," *Journal of the Optical Society of America-A*, vol. 2, no. 7, pp. 1160–1169, 1985.
- [5] D. Gabor, "Theory of communication," *Journal of the Institution of Electrical Engineers - Part III: Radio and Communication Engineering*, vol. 93, no. 26, pp. 429–457, 1946.
- [6] R. Gonzalez, "Improving phase correlation for image registration," in *Proc. of Image and Vision Computing New Zealand 2011*.
- [7] T. S. Lee, "Image representation using 2d gabor wavelets," *IEEE Trans. on Patterns analysis and Machine Intelligence*, vol. 18, no. 10, pp. 1–13, 1996.
- [8] S. Liao, and A. C. S. Chung, "Feature based nonrigid brain mr image registration with symmetric alpha stable filters," *IEEE Transaction on Image Processing*, vol. 29, no. 1, pp. 106–119, 2010.
- [9] H. Lin, P. Du, W. Zhao, L. Zhang, and H. Sun, "Image registration based on corner detection and affine transformation," *3rd International Congress on Image and Signal Processing*, vol. 5, pp. 2184–2188, 2010.
- [10] B. S. Manjunath and W. Y. Ma, "Texture features for browsing and retrieval of image data," *IEEE Transaction on Patterns analysis and Machine Intelligence*, vol. 18, no. 8, pp. 837–842, 1995.
- [11] R. Matungaka, Y.F. Zheng and R.L. Ewing, "Image Registration using Adaptive Polar Transform," *IEEE Transaction on Image Processing*, vol. 18, no. 10, pp. 2346–2354, 2009.
- [12] B. S. Reddy, and B. N. Chatterji, "An FFT-Based Technique for Translation, Rotation and Scale-Invariant Image Registration," *IEEE Transaction on Image Processing*, vol. 5, no. 8, pp. 1266–1271, 1996.
- [13] A. Roozgard, N. Barzigar, S. Cheng and P. Verma, "Medical image registration using sparse coding and belief propagation," *Engineering in Medicine and Biology Society (EMBC), 2012 Annual International Conference of the IEEE, IEEE*, pp. 1141–1144, 2012.
- [14] I. W. O. Serlie, F. M. Vos, R. Truyen, F. H. Post and L. J. V. Vliet, "Classifying CT image data into material fractions by a scale and rotation invariant edge model," *IEEE Transaction on Image Processing*, vol. 16, no. 12, pp. 2891–2904, 2007.
- [15] P. Thangavel and R. Kokila, "An Extension of FFT based image registration," in *Proc. Advances in computing and information technology*, vol. 2, pp. 729–737, 2012.
- [16] G. Tzimiropoulos, V. Argyriou, S. Zafeiriou and T. Stathaki, "Robust FFT-Based Scale-Invariant Image Registration with Image Gradients," *IEEE Transaction on Pattern Analysis and Machine Intelligence*, vol. 32, no. 10, pp. 1899–1906, 2010.
- [17] J. Wu, and A. Chung, "Multimodal brain image registration based on wavelet transform using SAD and MI," *Proc. of the Second International Workshop on Medical Imaging and Augmented Reality*, Springer Berlin Heidelberg, pp. 270–277, 2004.
- [18] FEI Face Database, <http://fei.edu.br/~cet/facedatabase.html>.
- [19] Medical Image Database, <http://www.midb.jp/db/en/>.

**R. Kokila** received her M.Sc and M.Phil from University of Madras during 2005 and 2006 respectively. She is pursuing Ph.D at University of Madras. Area of scientific interest: digital image processing and artificial neural networks.

**P. Thangavel** received his M.Tech and Ph.D. from Indian Institute of Technology and Bharathidasan University respectively. He is currently working as Professor and Head of the Department of Computer Science, University of Madras. Area of scientific interest: algorithms and artificial systems.